

1

:
 :
 43.9)
 1 , 1 , 1 , 14 19 (: =12:7,
 1 , 1 , 1 5 1 , 3 , 3 ,
 4 , 1 1.5 T
 , single shot spin echo EPI , b value (0, 1000)
 가
 10
 T1 T2 , FLAIR
 T1
 : 3 , 1 , 1
 (2) $1.15 \pm 0.13 (10^{-3} \text{ mm}^2/\text{s})$
 , (8) 2.84 ± 0.66 $3.10 \pm 0.16 (10^{-3} \text{ mm}^2/\text{sec})$
 :
 ,

가

(2, 3, 9)

(4 - 6, 11, 12).

(1).

가

가

2001	1	2003	7
------	---	------	---

19

가 12 , 가 7

6 79 (43.9)

15

¹가

2003 12 2

2004 3 31

,

4

. 14

3, 3, 1, 1, 2, 1, 1, 1, 5, 4, 1, 1.5 T MR (Gyrosan NT; Philips medical Systems, Best, The Netherlands) Quadrature head coil single shot spin echo EPI TR/TE = 4024/94(114) msec, 128 acquisition/256 reconstruction, 24 cm FOV, 5 mm thickness, 1 mm interslice gap, NSA =1. b value (0, 1000) b value 1000 (ADC map) 10 (region of interest) (partial volume effects) (Table 1). 19 15 가 3 15 (intra - 2 msec/10 msec, repetition time/ echo time) T2 (4500/100), FLAIR (6000/100 inversion time 2000) gadopentetate dimeglumine (Magnevist, Schering, Berlin, Germany) 0.1 mmol/Kg 1 (Fig. 2), 2 (Fig. 3) 4 3

Table 1. Diffusion -weighted Imaing Findings in 19 Patients with Intracranial Cystic Lesions

Patient number	Sex	Age	Location	Nature of lesion	Cystic component			Enhancement Pattern	ADC value (10 ⁻³ mm ² /sec)	Diagnosis
					T1	T2	DWI			
1	M	50	Lt.cerebellum	Single	-	+	+	Ring	1.15 ± 0.13	Bacterial abscess ^a
2	M	37	Lt.frontal lobe	Single	+	+	+	Ring	Not obtained	Bacterial abscess ^a
3	F	41	Lt.parieto-occipital lobe	Multiple	-	+	+	Irregular	0.80 ± 0.06	Bacterial abscess ^a
4	F	6	Rt.parieto-occipital lobe	Single	-	+	-	Nodular	Not obtained	Ependymoma ^a
5	M	53	Lt.parieto-occipital lobe	Multiple	-	+	-	Ring	Not obtained	Pilocytic astrocytoma ^a
6	F	17	Rt.frontal lobe	Single	-	+	-	Nodular	2.91 ± 0.15	Anaplastic astrocytoma ^a
7	F	37	Lt.parietal lobe	Single	-	+	-	Nodular	2.94 ± 0.26	Glioblastoma ^a
8	M	37	Lt.temporal lobe	Single	-	+	+/-	Irregular	Not obtained	Glioblastoma ^a
9	F	55	Rt.temporal lobe	Single	-	+	-	Nodular	3.09 ± 0.12	Glioblastoma ^a
10	M	43	Rt.cerebellum	Single	-	+	-	Nodular	3.08 ± 0.52	Hemangioblastoma ^a
11	M	32	Lt.cerebellum	Single	-	+	-	Nodular	3.10 ± 0.16	Hemangioblastoma ^a
12	M	58	Rt.cerebellum	Single	-	+	-	Nodular	Not obtained	Metastasis ^b
13	M	52	Rt.parietal lobe	Single	-	+	-	Irregular	2.95 ± 0.11	Metastasis ^b
14	M	67	Rt.parietal lobe	Single	-	+	-	Irregular	Not obtained	Metastasis ^b
15	M	40	Supratentorial, bilateral	Multiple	-	+	+	Ring	Not obtained	Metastasis ^b
16	F	26	Posterior fossa	Single	-	+	-	Not evident	2.84 ± 0.66	Arachnoic cyst ^b
17	M	79	Rt.temporal region	Single	-	+	-	Not evident	Not obtained	Arachnoid cyst ^a
18	F	68	Posterior fossa	Single	-	+	+	Not evident	Not obtained	Epidermoid ^a
19	M	36	Posterior fossa	Multiple	-	+	-	Nodular	3.06 ± 0.19	Schwannoma ^a

Signal intensities. T1 Signal: + white matter; - intermediate between white matter and CSF; - - equivalent CSF

T2 Signal: + + CSF; + intermediate between CSF and white matter. DWI Signal: - CSF, +/- parenchyma, + + hyperintensity

a: Histological diagnosis b: Clinical diagnosis

2
1
3
(palliative radiotherapy)
1
2
1.15 ± 0.13, 0.80 ±
0.64 (10⁻³ mm²/sec)
0.66 3.10 ± 0.16 (10⁻³ mm²/sec)
2.84 ±
T1
T2
3
1
1
(extra - axial)
4
3
1
1
가
가
가
가

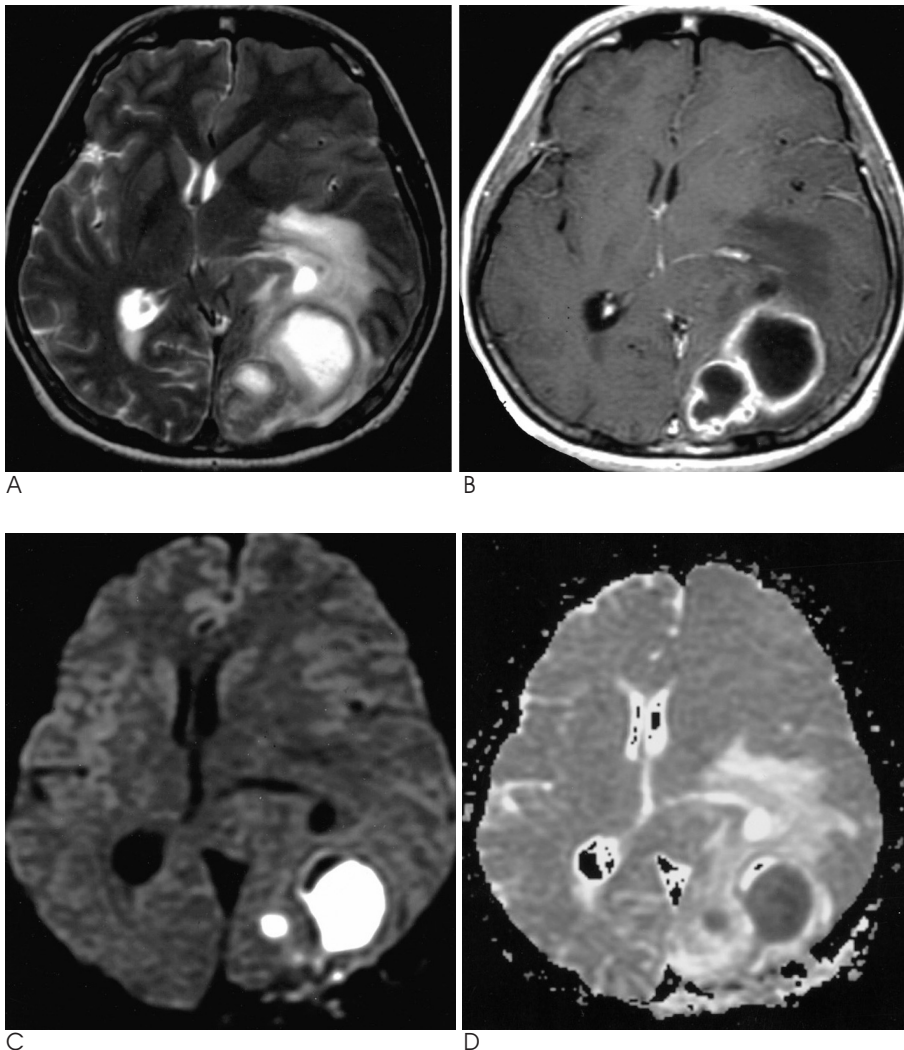


Fig. 1. 41-year-old female with surgically proven bacterial abscess in left occipital lobe (patient 3).

A. Axial T2-weighted MR image (TR/TE, 2000/90) shows markedly hyperintense abscess cavities with hypointense capsule and hyperintense surrounding edema.

B. Contrast enhanced axial T1-weighted image (TR/TE, 550/20) shows hypointense abscess cavities with enhanced abscess capsule and hypointense surrounding edema.

C. Diffusion-weighted image shows markedly high signal intensity of abscess cavities.

D. Abscess has marked low signal intensity on apparent diffusion coefficient (ADC) map image; mean ADC was 0.80 (± 0.06 10⁻³ mm²/sec).

가

(1).

가 , (pus)

가 in vitro (debris)

(cellularity) 가 ,

Ebisu , (streptococcus intermedius)

가 (fibrinogen)

($0.31 \times 10^{-3} \text{ mm}^2/\text{s}$)

(4). (5)

(18).

가

가 (19).

1

Lai (7)

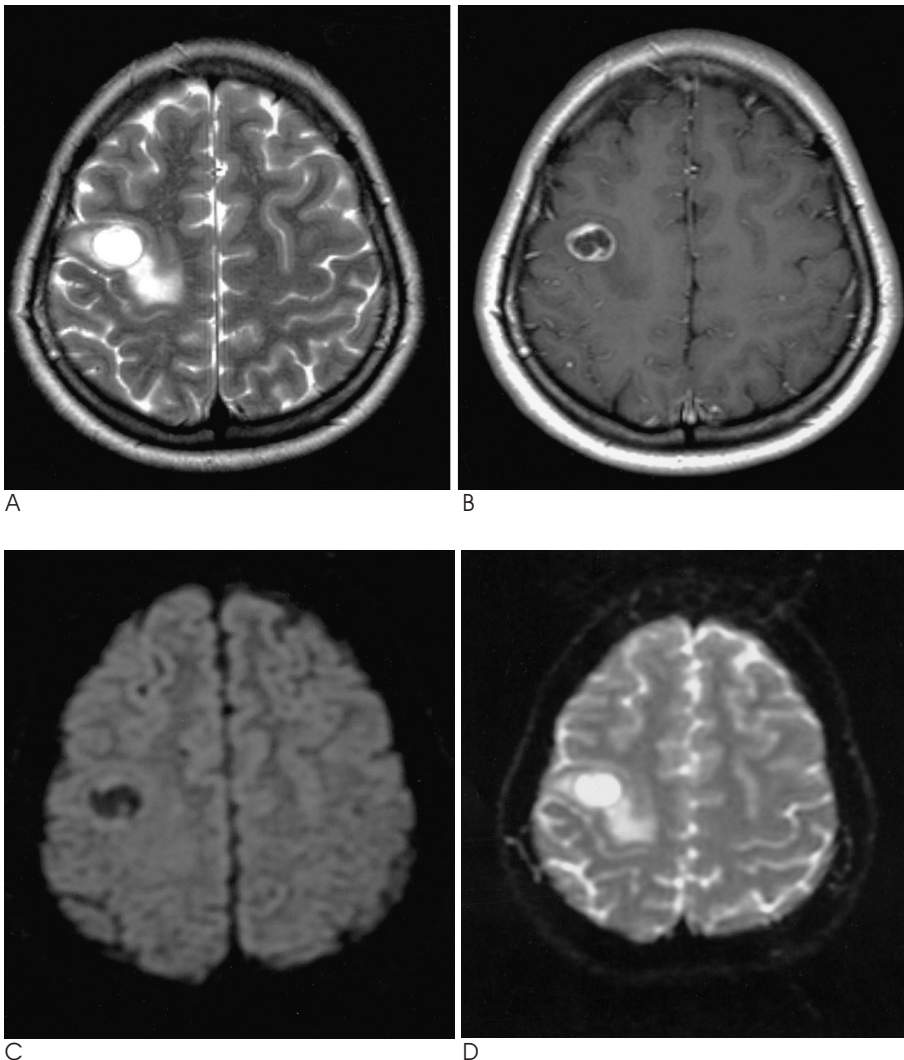


Fig. 2. 17-year-old female with surgically proven anaplastic astrocytoma in right frontal lobe (patient 6).

A. Axial T2-weighted MR image (TR/TE, 2000/90) shows thin, isointense border and necrotic, strongly hyperintense central region with adjacent edema.

B. Contrast enhanced axial T1-weighted image (TR/TE, 550/20) shows nodular enhancement of solid border with hypointense central region.

C. Diffusion-weighted image shows markedly hypointense tumor cavity, slightly hyperintense enhancing wall.

D. Apparent diffusion coefficient (ADC) map image shows markedly increased signal in mass compared with that in cerebrospinal fluid; mean ADC was $2.91 (\pm 0.15, 10^{-3} \text{ mm}^2/\text{sec})$.

.
 , Tung
 $0.28 - 0.70 \text{ } (10^{-3} \text{ mm}^2/\text{sec})$
 $0.79 \text{ } (10^{-3} \text{ mm}^2/\text{sec})$
(8). 가 $1.15 \pm 0.13 \text{ } (10^{-3}$

가
(8, 10, 20). 가
mm²/sec)
Ketelslegers
(16).

,
(creamy pus)
(22).
T1
가
가
. 가
가
(21).
(6, 14, 16)

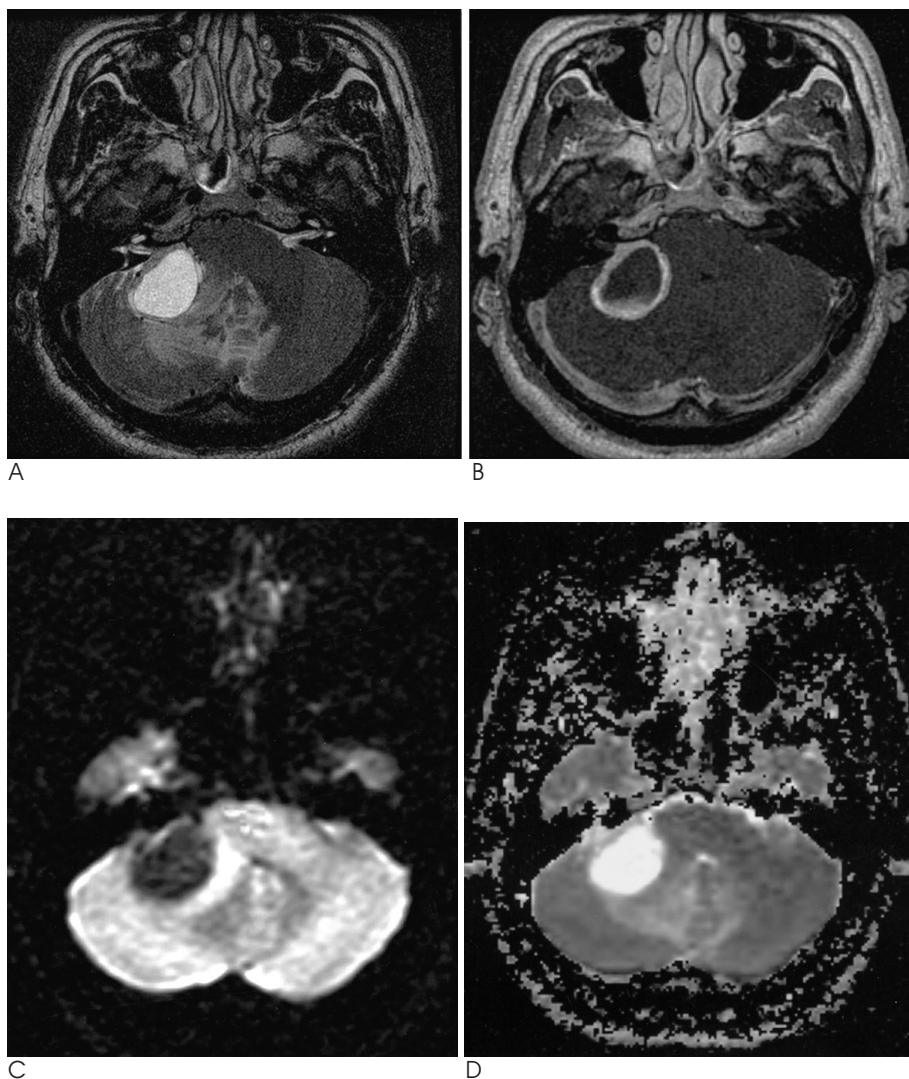


Fig. 3. 43-year-old man with surgically proven hemangioblastoma in right cerebellar hemisphere (patient 10).

A. Axial T2-weighted MR image (TR/TE, 2000/90) shows isointense solid border surrounds a necrotic, strongly hyperintense central region and hyperintense adjacent edema.

B. Contrast enhanced axial T1-weighted image (TR/TE, 550/20) shows diffuse nodular enhancement of solid border, sparing the hypointense necrotic portion.

C. Diffusion-weighted image shows markedly hypointense tumor cavity.

D. ADC map image shows marked hyperintense signal in right cerebellar hemispheric mass ; mean ADC was $3.08 (\pm 0.52, 10^{-3} \text{ mm}^2/\text{sec})$.

(13, 15, 17),

가

(7, 14).

T2

(21).

ADC

가

가

(16).

1. Osborn AG. *Pyogenic Parenchymal Infections*. In: Osborn AG, Ed. *Diagnostic Neuroradiology*. St.Louis, MO: Mosby Year-Book;1994: 688-692
2. Moseley ME, Cohen Y, Kucharczyk J, et al. Diffusion-weighted MR imaging of anisotropic water diffusion in cat central nervous system. *Radiology* 1990;176: 439 - 445
3. . Single shot EPI 1998;39:7-13
4. Ebisu T, Tanaka C, Umeda M, et al. Discrimination of brain abscess from necrotic or cystic tumors by diffusion-weighted echo planar imaging. *Magn Reson Imaging* 1996;14:1113-1116
5. Kim YJ, Chang KH, Song IC, et al. Brain abscess and necrotic or cystic brain tumor: discrimination with signal intensity on diffusion-weighted MR imaging. *AJR Am J Roentgenol* 1998;171:1487-1490
6. Desprechins B, Stadnik T, koerts G, Shabana W, Breucq C, Osteaux M. Use of diffusion-weighted MR imaging in differential diagnosis between intracerebral necrotic tumors and cerebral abscesses. *AJNR Am J Neuroradiol* 1999;20:1252-1257
7. Lai PH, Ho JT, Chen WL, et al. Brain abscess and necrotic brain tumor: discrimination with proton MR spectroscopy and diffusion-

weighted imaging. *AJNR Am J Neuroradiol* 2002;23:1369-1377

8. Tung GA, Evangelista P, Rogg JM, Duncan JA 3rd. Diffusion-weighted MR imaging of rim-enhancing brain masses: is markedly decreased water diffusion specific for brain abscess? *AJR Am J Roentgenol* 2001;177:709-712
9. Okamoto K, Ito J, Ishikawa K, Sakai K, Tokiguchi S. Diffusion-weighted echo-planar MR imaging in differential diagnosis of brain tumors and tumor-like conditions. *Eur Radiol* 2000;10:1342-1350
10. Holtas S, Geijer B, Stromblad LG, Maly-Sundgren P, Burtscher IM. A ring-enhancing metastasis with central high signal on diffusion-weighted imaging and low apparent diffusion coefficients. *Neuroradiology* 2000;42:824-827
11. Krabbe K, Gideon P, Wagn P, Hansen U, Thomsen C, Madsen F. MR diffusion imaging of human intracranial tumors. *Neuroradiology* 1997;39:483-489
12. Maeda M, Kawamura Y, Tamagawa Y, et al. Intravoxel incoherent motion (IVIM) in intracranial, extraaxial tumors and cysts. *J Comput Assist Tomogr* 1992;16:514-518
13. Steffey DJ, De Filipp GJ, Spera T, Gabrielsen TO. MR imaging of primary epidermoid tumors. *J Comput Assist Tomogr* 1988;12:438-440
14. Noguchi K, Watanabe N, Nagayoshi T, et al. Role of diffusion-weighted echo-planar MRI in distinguishing between brain abscess and tumor: a preliminary report. *Neuroradiology* 1999;41:171-174
15. Dechambre S, Duprez T, Lecouvet F, Raftopoulos C, Gosnard G. Diffusion-weighted MRI postoperative assessment of an epidermoid tumour in the cerebellopontine angle. *Neuroradiology* 1999; 41:829-831
16. Ketelslegers E, Duprez T, Ghariani S, Thauvoy C, Cosnard G. Time dependence of serial diffusion-weighted imaging features in a case of pyogenic brain abscess. *J Comput Assist Tomogr* 2000;24: 478-481
17. Tsuruda JS, Chew WM, Moseley ME, Norman D. Diffusion-weighted MR imaging of the brain: value of differentiating between extraaxial cysts and epidermoid tumors. *AJNR Am J Neuroradiol* 1990;11:925-931
18. Rusakov DA, Kullman DM. Geometric and viscous components of the tortuosity of the extracellular space in the brain. *Proc Natl Acad Sci U.S.A.* 1998;95:8975-8980
19. Tien RD, Felsberg GJ, Friedman H, Brown M, MacFall J. MR imaging of high-grade cerebral gliomas: value of diffusion-weighted echoplanar pulse sequences. *AJR Am J Roentgenol* 1994;162:671-677
20. Hartmann M, Jansen O, Heiland S, Sommer C, Munkel K, Sartor K. Restricted diffusion within ring enhancement is not pathognomonic for brain abscess. *AJNR Am J Neuroradiol* 2001;22:1738-1742
21. Guo AC, Provenzale JM, Cruz LC Jr, Petrella JR. Cerebral abscesses: investigation using apparent diffusion coefficient maps. *Neuroradiology* 2001;43:370-374
22. Monabati A, Kumar P, Kamkarpour A. Intraoperative cytodiagnosis of metastatic brain tumors confused clinically with brain abscess. A report of three cases. *Acta Cytol* 2000;44:437-441

The Usefulness of Diffusion Weighted Imaging in the Differential Diagnosis of Various Intracranial Cystic Lesions¹

Yon Kwon Ihn, M.D., Jeong Su Jun, M.D., Seong Su Hwang, M.D.,
Jun Hyun Baik, M.D., Young Ha Park, M.D.

¹Department of Radiology, College of Medicine, The Catholic University of Korea

Purpose: The purpose of this study was to evaluate the usefulness of diffusion-weighted imaging (DWI) for the differential diagnosis of various intracranial cystic lesions.

Materials and Methods: This study included 19 patients (13 males, 6 females) with a mean age of 42.5 years. The final histopathological diagnoses for 14 patients were pyogenic brain abscess ($n=3$), glioblastoma ($n=3$), ependymoma ($n=1$), anaplastic astrocytoma ($n=1$), pilocytic astrocytoma ($n=1$), hemangioblastoma ($n=2$), arachnoid cyst ($n=1$), epidermoid ($n=1$) and schwannoma ($n=1$). The other cases of metastasis ($n=4$) and arachnoid cyst ($n=2$) were diagnosed on the basis of clinical, laboratory and imaging data. DWI imaging studies were performed with a 1.5 T MR system. A single shot spin echo EPI pulse sequence was applied. B values were set at 0 and 1000 sec/mm². The apparent diffusion coefficient (ADC) were calculated from the ADC map of 10 different cystic brain lesions. Conventional MR imaging included T2WI, T1WI, FLAIR and contrast enhanced T1WI. We analyzed the location, nature, signal intensity on DWI, and the enhancement pattern of the lesions.

Results: All of the 3 cases of brain abscess, 1 of 4 cases of metastasis and 1 case of epidermoid showed hyperintensity on DWI. The mean ADC value of brain abscess (2 cases) was less than 1.15 (0.13×10^{-3} mm²/s). The mean ADC values of the other cystic lesions (8 cases) were variable, ranging from 2.840.66 to 3.100.16 (10^{-3} mm²/sec).

Conclusion: DWI and ADC values were useful in the differential diagnosis of various intracranial cystic lesions, but some metastatic tumors may mimic a brain abscess on DWI. Therefore, a clinical correlation is mandatory.

Index words : Magnetic resonance (MR), diffusion
Brain, abscess

Address reprint requests to : Yon Kwon Ihn, M.D., Department of Radiology, St. Vincent 's Hospital, College of Medicine,
The Catholic University of Korea, 93-1 Ji-dong, Paldal-gu, Suwon-si, Gyenggi-do 442-723, Korea.
Tel. 82-31-249-7486 Fax. 82-31-247-5713 E-mail: Ihn@catholic.ac.kr